PROC. INST. ACOUSTICS VOL 7 PT 3 1985

NUMERICAL SIMULATIONS OF THE DEGRADATION OF ARRAY DIRECTIVITY DUE TO SCATTERING

Peter F. Dobbins and Colin Schofield

British Aerospace,
Underwater Research and Engineering Unit, Weymouth, UK.

INTRODUCTION

The problem to be considered is the degradation of the directivity pattern of a linear receiving array due to scattering in a random transmission medium. Many authors, eg.[1,2], have investigated the effects of random variations in the phase and amplitude sensitivities of radio and sonar arrays but in this case, where the phase and amplitude fluctuations are due to distortion of the propagating wavefront by the medium, the variations are partially correlated along the line of the array.

Theoretical expressions for the time-averaged beampattern [3,4] of a line array in the presence of correlated phase and amplitude fluctuations as well as its variance [5] have been given previously, but to date this theory has no experimental confirmation. Before performing experiments to provide such confirmation, a series of computer simulations has been carried out, based on a conventional beamforming algorithm and using signal fluctuations representative of those expected in the ocean when scattering is caused by a temperature microstructure.

Examples of statistical results from these simulations are presented and good agreement with the theoretical predictions is demonstrated. The potential advantages of the simulation technique over the theoretical approach are also discussed.

THEORETICAL ARRAY PERFORMANCE

An analytical expression for the effect of correlated phase fluctuations on the time-averaged directivity pattern of a line array was first derived by Berman and Berman [3]. By assuming that the correlation of the signal fluctuations between elements of the array depends only on their separation, Lord and Murphy [4] simplified the Bermans' equation and also included the effect of amplitude fluctuations.

Because phase fluctuations have a more dramatic effect on the array response than amplitude fluctuations, phase only will be considered in the examples that follow.

In this case the expected mean square beampattern is [4]

$$E[\langle Y^2\rangle] = \frac{2}{N^2}\left\{\frac{N}{2} + \sum_{n=1}^{N-1}(N - n)\cos(n\gamma)\exp[\langle\phi^2\rangle(\rho(nd) - 1)]\right\} \qquad (1)$$

where N is the number of elements in the array,
d is the separation between elements,
$\langle\phi^2\rangle$ is the mean square phase fluctuation,
$\rho(nd)$ is the phase correlation at separation nd
and $\gamma = kd\sin\theta$, with acoustic wavenumber $k = 2\pi/\lambda$.
θ is the bearing angle relative to the array normal.

The variance in the expected pattern was derived by Brown [5] and is given by

$$V[\langle Y^2\rangle] = \frac{1}{N^4}\sum_{n=1}^{N-1}\sum_{m=n+1}^{N}\sum_{j=1}^{N-1}\sum_{k=j+1}^{N}\exp[\langle\phi^2\rangle\{\rho(|m-n|d) + \rho(|j-k|d) - 2\}]$$

$$\times \left\{\cos[(n-m-j+k)\gamma](\exp[\langle\phi^2\rangle R] - 1)\right. \qquad (2)$$

$$\left. + \cos[(n-m+j-k)\gamma](\exp[-\langle\phi^2\rangle R] - 1)\right\}$$

where

$$R = \rho(|j-n|d) - \rho(|j-m|d) + \rho(|m-k|d) - \rho(|n-k|d) \qquad (3)$$

Fig.1 gives an example of the use of these equations. The solid line shows the ideal beampattern of a 10 element uniform line array, with $\lambda/2$ spacing, at 10kHz. The dashed line is the average pattern with a mean square phase variation of 1 radian and a correlation function as described in the following section. The dotted line shows the average plus three standard deviations, which represents the maximum level to be expected.

The scale size of the correlation function in this example is 0.6m, which is comparable with the array length of 0.675m. The results obtained depend strongly on this ratio of the correlation scale to the array length.

THE MEDIUM

In order to estimate the level of phase fluctuations to be expected and the associated correlation function, it is necessary to consider the properties of the medium and their effect on sound propagation.

There are many scattering mechanisms in the ocean, and their relative importance depends on the acoustic frequency and the propagation range. In this study the interest was in high frequency short range propagation and under these conditions, neglecting transient phenomena such as fish and bubbles, the most significant contributor to scattering is the temperature microstructure.

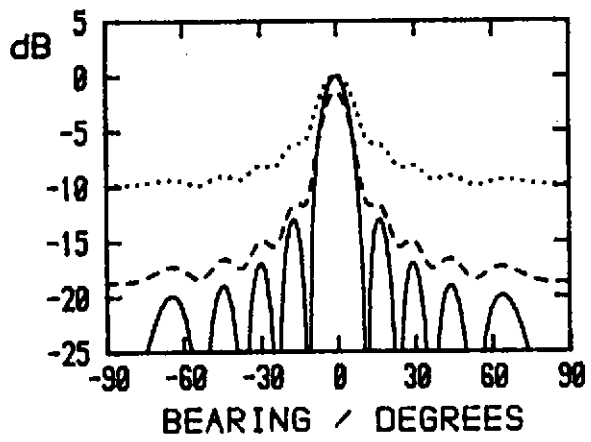

Fig.1 Ideal pattern (solid line), 10 element 10kHz array: average (dashed) and av + 3 std.dev. (dotted) for 1rad rms phase variation, scale 0.6m

This microstructure can be modelled by an empirical one-dimensional spatial wavenumber spectrum of the refractive index, formulated by Medwin [6] from measurements in the upper ocean and shown in Fig.2.

This model is based on the concept that temperature, and hence refractive index, is a passive contaminant of the turbulent water motion. The idealised form of the spectrum, $\Phi(\kappa)$, outlined by the discontinuous straight lines, is divided into 4 ranges, separated by the wavenumbers κ_m, κ_t and κ_o.

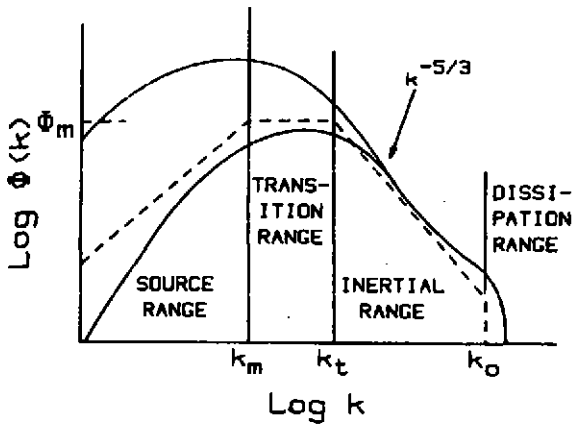

Fig.2 Typical measured wavenumber spectra for refractive index (solid lines) and idealised form (dashes).

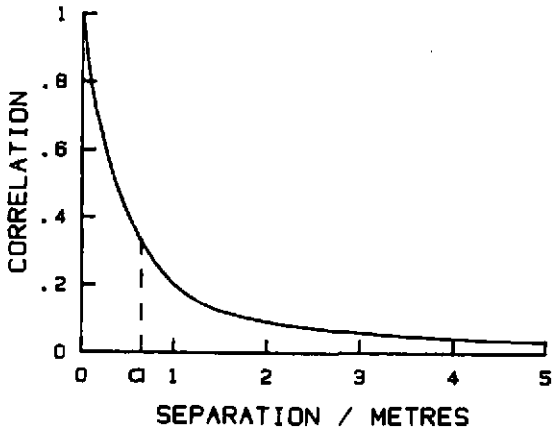

Fig.3 Spatial correlation function of refractive index computed from idealised spectrum of Fig.2.

Kinetic energy is put into the source range by forces of winds, tides, currents and so on; the inertial range contains the turbulent eddies which obey a five-thirds power law; the transition range is an arbitrary bridge between the source range and inertial range; in the dissipative range energy is dissipated by viscosity and temperature fluctuations are smoothed by diffusion. Medwin assumed that the spectrum was truncated below κ_m and κ_o.

The general equation for the spectrum is [6]

$$\Phi(\kappa) = \begin{cases} 0 & \kappa \leq \kappa_m \\ \Phi_m & \kappa_m < \kappa \leq \kappa_t \\ \Phi_m(\kappa/\kappa_t)^{-5/3} & \kappa_t < \kappa \leq \kappa_o \\ 0 & \kappa > \kappa_o \end{cases} \qquad (4)$$

Φ_m is related to the mean square refractive index fluctuation $\langle\mu^2\rangle$ by

$$\Phi_m = 2\langle\mu^2\rangle/5\kappa_t \qquad (5)$$

and the boundary wavenumbers are given by

$$\kappa_m = (\pi/2)(1/d + 1/(h - d)) \qquad (6)$$

$$\kappa_o = (3n/2)^{-3/4}(\varepsilon/D^3)^{1/4} \qquad (7)$$

$$\kappa_t = 0.5(\kappa_m\kappa_o)^{1/2} \qquad (8)$$

where d is the observer depth, h is the total water depth, n is a dimensionless constant generally taken as 0.59, ε is the rate of kinetic energy dissipation per unit mass and D is thermal diffusivity.

The spatial correlation function of the refractive index fluctuations, $C_\mu(r)$, is obtained from the spectrum using the Fourier transform relationship:

$$C_\mu(r) = \frac{1}{\langle\mu^2\rangle}\int_0^\infty \frac{\sin\kappa r}{\kappa r}\,\Phi_\mu(\kappa)d\kappa \qquad (9)$$

where r is spatial separation.

Fig.3 shows a typical correlation function, calculated for an observer depth of 100m and a water depth of 200m. The mean scale size of the temperature inhomogeneities, a, is given by

$$a = \int_0^\infty C_\mu(r)dr \qquad (10)$$

and in the example, Fig.3, a is 0.6m which is in general agreement with published experimental data.

There is no similar model for predicting the level of temperature fluctuations, but it is generally found that the mean square refractive index variation is in the order of 10^{-8}.

PROPAGATION

There exist many theoretical treatments of wave propagation in random media, but there is much experimental evidence to support the single scatter theories described, for example, in the books by Tatarski [7] and Chernov [8]. The conditions necessary for these theories, which rely on small scattering angles, are that both the inhomogeneity scale size and propagation range be large compared with the acoustic wavelength, and that the range be greater than the Fresnel distance associated with the inhomogeneities and less than the distance at which multiple scattering occurs.

These conditions are expressed as

$kz >> 1$	(range)	(11)
$ka >> 1$	(scale size)	(12)
$4z/ka^2 >> 1$	(Fresnel distance)	(13)
$z < 1/(k^2\langle\mu^2\rangle a)$	(single scattering)	(14)

and within these limits the mean square phase fluctuation is

$$\langle\phi^2\rangle = \langle\mu^2\rangle k^2 z a \qquad (15)$$

and the correlation function of the phase fluctuations transverse to the propagation direction is identical to that of the refractive index variations, whilst along the direction of propagation the fluctuations are essentially completely correlated.

A worst case estimate of the level of phase fluctuations may be obtained by setting the range equal to the multiple scattering distance, and by combining eqs(14) and (15) the mean square fluctuation is found to be 1 radian. This is the value that will be used in the examples. In practice the multiple scattering range varies from about 100km at 10kHz down to 10m at 1MHz.

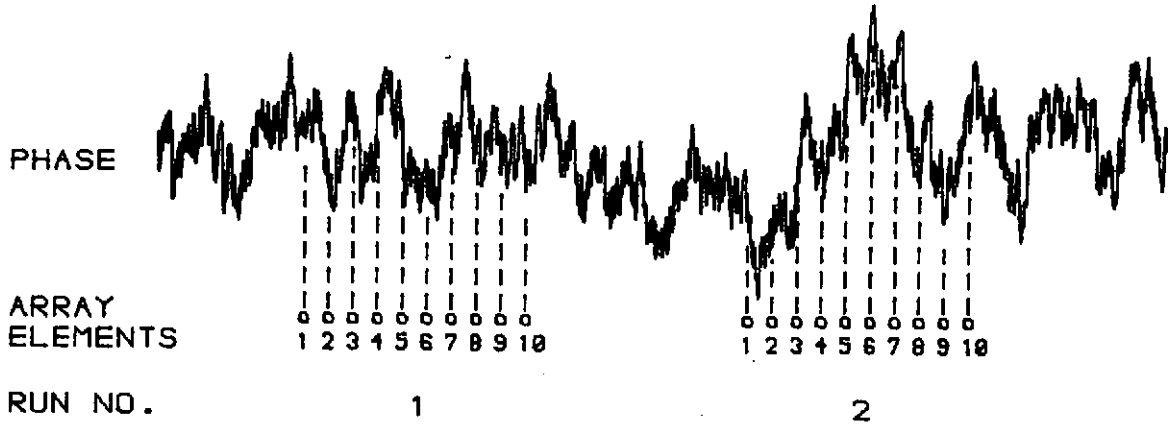

Fig.4 Phase variation at each array element is obtained by interpolating between data points in a random phase file. A new section of phase data is used for each realisation of the beampattern.

BEAMPATTERN SIMULATION

The amplitude of the output from an N-element uniform line array, having no shading or steering corrections, in response to a signal incident from direction θ is

$$Y(\theta) = \frac{1}{N}\left|\sum_{n=1}^{N}(\cos\psi_n + i\sin\psi_n)\right| \qquad (16)$$

$$\psi_n = nkd\sin\theta + \phi_n \qquad (17)$$

where ϕ_n is the phase deviation at the nth element.

To carry out the simulations, data representing the phase variations in the incident wavefront were generated using a method described by Buckley [9]. The appendix to Buckley's paper gives a numerical method for combining any power spectrum or correlation function with a set of uniformly distributed random numbers. The result is a random series, corresponding to a specified distance in the medium, with a Gaussian distribution and having the required correlation function.

For each simulation the values of the ϕ_n are taken from a small portion of the phase data which represents a length equivalent to that of the array. The phase at each element is linearly interpolated between the phase data points as shown schematically in Fig.4.

Subsequent simulations can then be performed by moving the starting point of the array to a new position within the phase data file, thereby using a new length of phase disturbance information. This new position may be at a fixed interval through the file, at a random interval or even within another independent file of phase data.

A typical sequence of beampatterns obtained in this manner is shown in Fig.5. These are part of a set used in producing the example results in the following section, and the parameters used will be given there.

It was noted in the previous section that the transverse phase correlation

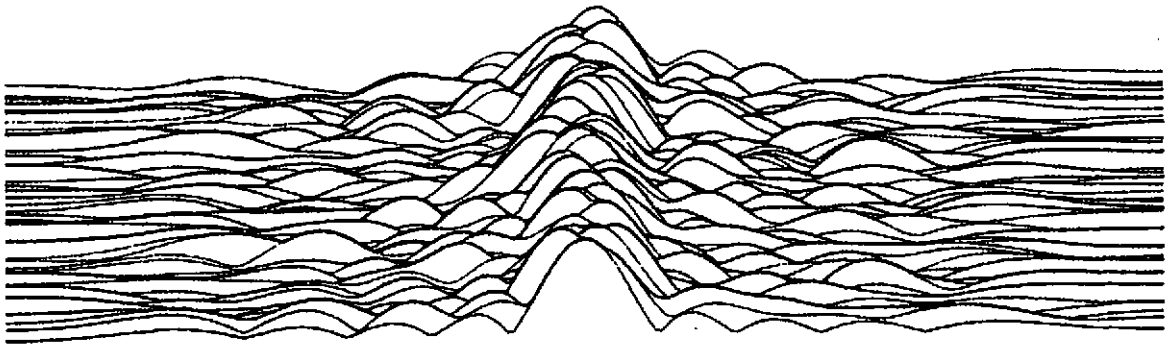

Fig.5 Typical sequence of simulated beampatterns, plotted on a linear scale. Array details and phase fluctuation statistics are as in Fig.1.

function should be identical to that of the temperature fluctuations but that along the line of propagation the phase fluctuations are completely correlated. This variation is easily incorporated in both the theory and the simulation, but the effect is small and only noticeable at large bearing angles so, to save computing time, the change of correlation with bearing has been neglected in these examples.

EXAMPLE RESULTS

Typical results are presented in Fig.6. As in Fig.1 these are for a 10-element uniform line array with $\lambda/2$ spacing. In each case the mean square phase fluctuation is 1 radian and the correlation function is as shown in Fig.3.

Frequencies used are 1kHz, 10kHz and 100kHz, giving array lengths of 6.75m, 0.675m and 0.0675m which are respectively greater than, comparable with and smaller than the correlation scale of the phase fluctuations. The sequence of beampatterns shown in Fig.5 are at 10kHz.

Figs.6a, 6b and 6c show the average responses at 1kHz, 10kHz and 100kHz respectively. The solid lines are the theoretical predictions, eq(1), and the dashed lines are the averages computed from 100 realisations of the simulated beampattern. The phase data were taken from a random position in the phase file for each realisation.

Figs.6d, 6e and 6f are for 1kHz, 10kHz and 100kHz respectively. The solid lines show the theoretical average plus three standard deviations from eqs(2) and (3) and the dashed lines are computed from 100 realisations, as in the case of the averages. For comparison the dotted lines show the maximum levels achieved throughout the simulation run.

DISCUSSION

The good general agreement between the theory and simulations can be seen from Fig.6, and this gives confidence in the results, but it is noted firstly that the agreement is less good in the lower frequency examples and secondly that results are not as good for the variance as for the average response.

The reason for the discrepancy at low frequencies is that the length of the array - 6.75m at 1kHz - is comparable with the equivalent length of the phase data file - 10m in these examples - and it is not possible to obtain a large number of statistically independent sections of phase data. Results can be improved by generating a new set of phase data for each realisation of the

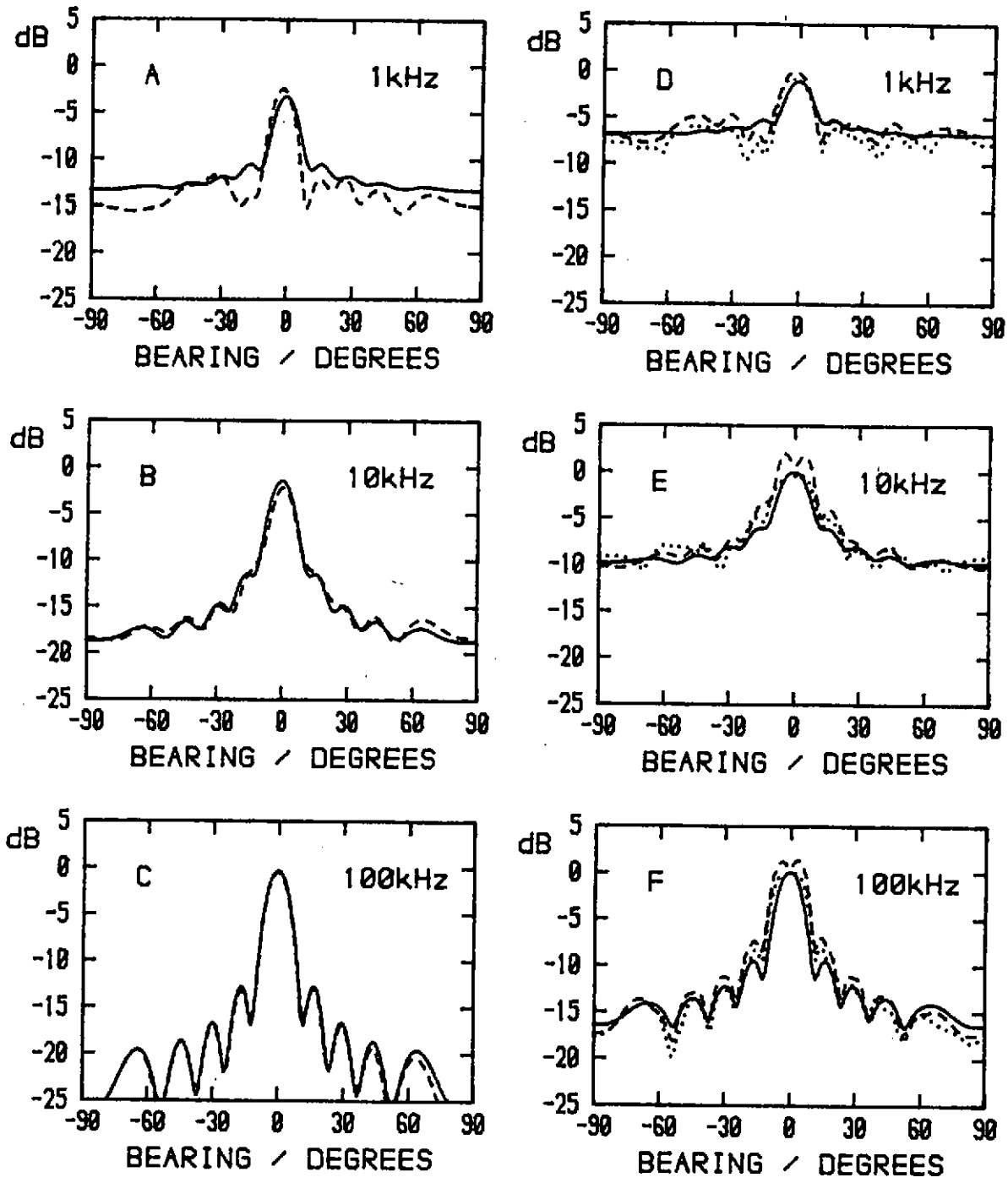

Fig.6 Results for 10 element array with 1 rad. rms phase fluctuation, correlation scale 0.6m: average beampatterns (a,b,c) and average plus 3 std.dev (e,d,f). Solid lines are theory, dashed lines are simulation statistics and dotted lines are maximum simulation levels achieved.

beampattern, but at the expense of considerably increased computing time.

The discrepancies in the variance are mainly because both the theoretical estimate of variance and the use of average plus three standard deviations as a measure of the maximum level assume a Gaussian distribution, whereas the distributions found in the simulations are skewed towards a low level at bearings where the average array output is high and skewed towards a high level where the array output is low. As can be seen from the examples, this means that the theoretical estimates of both average and variance tend to be low where the array output is high and vice versa. This effect is compounded when the average and variance are combined in the plots of average plus three standard deviations.

Better agreement in the results is possible by increasing the number of realisations used, but an order of magnitude increase is necessary to gain a significant improvement. 100 realisations were used for these examples to make the time taken comparable with that required to evaluate the theoretical equations. Computing the theoretical average presents no problems but the variance, eqs(2) and (3), requires the evaluation of a quadruple summation and the time taken is proportional to the fourth power of the number of elements in the array. The theoretical results for the examples took about 50 seconds each on a VAX 11/780, so an array of 100 elements would have taken about 6 days! The time taken for the simulations, however, is simply proportional to the number of elements and the number of realisations. 100 realisations of 100 elements takes less than 10 minutes.

Although the examples were produced on a large computer, the simulation procedure is quite practicable using a desk-top computer; the programs were originally developed on a small machine. The time needed to evaluate the theoretical equations becomes ridiculous on a desk-top with arrays of more than about 10 elements.

The other advantages of the simulation technique are firstly that the array may be shaded or steered or have non-uniform spacing - the theory only applies to uniform broadside arrays - and secondly that statistics may be computed for which analytical results are not available. Examples include the variation of the beam pointing direction and the average beamwidth. These additional statistics make it possible to estimate, for instance, the probability of detecting a target in the nominal beampointing direction, information which is useful in evaluating a practical sonar system.

CONCLUSIONS

The examples presented show that the statistics obtained from simulations of beampatterns with correlated phase fluctuations are in agreement with theoretical estimates of the average directivity pattern and its variance, which, in the absence of experimental evidence, gives confidence in the results. The number of realisations used for the simulations were within the capability of a desk-top computer, and the simulation technique has the advantages that less computer time is required for large arrays than is needed to evaluate the theoretical equations and that statistical results may be computed for which no analytical expression is available.

ACKNOWLEDGMENT

This work was supported by the Procurement Executive, the Ministry of Defence.

REFERENCES

[1] D.J. Ramsdale and R.A. Howerton, 'Effects of Element Failure and Random Errors in Phase and Amplitude on the Sidelobe Level Attainable with a Linear Array', J.A.S.A., 68(3), 901-906 (1980)

[2] A.H. Quazi, 'Array Beam Response in the Presence of Amplitude and Phase Fluctuations', J.A.S.A., 72(1), 171-180 (1982)

[3] H.G. Berman and A. Berman, 'Effect of Correlated Phase Fluctuations on Array Performance', J.A.S.A., 34(5), 555-562 (1962)

[4] G.E. Lord and S.R. Murphy, 'Reception Characteristics of a Linear Array in a Random Transmission Medium', J.A.S.A., 36(5), 850-854 (1964)

[5] J.L. Brown, 'Variation of Array Performance with Respect to Statistical Phase Fluctuations', J.A.S.A., 34(12), 1927-1928 (1962)

[6] H. Medwin, 'Sound Phase and Amplitude Fluctuations due to Temperature Microstructure in the Upper Ocean', J.A.S.A., 56(4), 1105-1110 (1974)

[7] V.I. Tatarski, 'Wave Propagation in a Turbulent Medium', Trans. R.A. Silverman, McGraw-Hill (1961)

[8] L.A. Chernov, 'Wave Propagation in a Random Medium', Trans. R.A. Silverman, McGraw-Hill (1960)

[9] R. Buckley, 'Diffraction by a Random Phase-Changing Screen: A Numerical Experiment', J. Atmos. and Terr. Phys., 37(11), 1431-1446 (1975)